Epigenetically regulated PCDHB15 impairs aggressiveness of metastatic melanoma cells

Arnaud Carrier, Cécile Desjobert, Valérie Lobjois, Lise Rigal, Florence Busato, Jörg Tost, Miquel Ensenyat-Mendez, Diego M Marzese, Anne Pradines, Gilles Favre, et al.

Epigenetically regulated *PCDHB15* impairs aggressiveness of metastatic melanoma cells

Arnaud Carrier[1,2], Cécile Desjobert[1], Valérie Lobjois[3'4], Lise Rigal[3], Florence Busato[5], Jörg Tost[5], Miquel Ensenyat-Mendez[6], Diego M. Marzese[6], Anne Pradines[7,8], Gilles Favre[7,8], Laurence Lamant[9], Luisa Lanfrancone[10], Chantal Etievant[1], Paola B. Arimondo[1,11 *,] Joëlle Riond[1,7*]

1. Unité de Service et de Recherche USR n°3388 CNRS-Pierre Fabre, Epigenetic Targeting of Cancer (ETaC), Toulouse, France
2. Cancer Epigenetics Group, Institut de Recerca Contra la Leucèmia Josep Carreras, Barcelona, Spain
3. Institut des Technologies Avancées en Sciences du Vivant – ITAV-USR3505, Université de Toulouse, CNRS, Université Paul Sabatier-UT3, Toulouse, France
4. Laboratoire de Biologie Cellulaire et Moléculaire du Contrôle de la Prolifération, CNRS UMR 5088, Université Paul Sabatier-UT3, Toulouse, France
5. Laboratory for Epigenetics and Environment, Centre National de Recherche en Génomique Humain, CEA-Institut de Biologie Francois Jacob, Université Paris-Saclay, Evry, France
6. Cancer Epigenetics Laboratory at the Cancer Cell Biology Group, Institut d'Investigació Sanitària Illes Balears (IdISBa), Palma, Spain
7. Université de Toulouse, Inserm, CNRS, Université Toulouse III-Paul Sabatier, Centre de Recherches en Cancérologie de Toulouse, Toulouse, France
8. Laboratoire de Biologie Médicale Oncologique, Institut Claudius Regaud, Institut Universitaire du Cancer de Toulouse-Oncopole, Toulouse, France
9. Laboratoire d'Anatomopathologie, Institut Universitaire du Cancer Toulouse Oncopole, Toulouse, France.
10. Instituto Europeo di Oncologia, Department of Experimental Oncology, Via Adamello 16, 20139 Milan, Italy
11. EpiCBio, Epigenetic Chemical Biology, Department Structural Biology and Chemistry, Institut Pasteur, CNRS UMR n°3523, 28 rue du Dr Roux, 75015 Paris, France

* The authors share last co-authorship and correspondence is to be addressed to them: joelle.riond@inserm.fr and paola.arimondo@cnrs.fr

The authors state no competing interests.

Running title: *PCDHB15* impairs aggressiveness of metastatic melanoma cells

Keywords: DNA methylation, aggressiveness, melanoma, tumor suppressor, protocadherin

Abstract

The protocadherin proteins are cell adhesion molecules at the crossroad of signaling pathways playing a major role in neuronal development. It is now understood that their role as signaling hubs is not only important for the normal physiology of cells but also for the regulation of

hallmarks of cancerogenesis. Importantly, protocadherins form a cluster of genes that is regulated by DNA methylation. We have identified for the first time that *PCDHB15* gene is DNA hypermethylated on its unique exon in the metastatic melanoma-derived cell lines and patients' metastases compared to primary tumors. This DNA hypermethylation silences the gene, and treatment with the DNA demethylating agent 5-aza-2'-deoxycytidine reinduces its expression. We explored the role of *PCDHB15* in melanoma aggressiveness and showed that over-expression impairs invasiveness and aggregation of metastatic melanoma cells *in vitro* and formation of lung metastasis *in vivo*.

These findings highlight important modifications of the methylation of the *PCDH*β genes in melanoma and support a functional role of *PCDHB15* silencing in melanoma aggressiveness.

Introduction

Melanoma is a type of cancer with increasing incidence [1] and, until recently, was often fatal once it metastasized to distant organs. New therapeutic approaches, including the molecular targeting of activated oncogenes and immune-based therapies, even in patients with advanced disease [2]. Nevertheless, many patients develop therapy resistance or do not respond to treatment. Therefore, the identification of molecular traits underpinning melanoma aggressiveness remains an ongoing challenge not only to improve treatment, but also to improve diagnosis and prognosis [3].

Besides the activating mutations in the *BRAF* and *NRAS* oncogenes, found in significant proportions of primary melanomas, important epigenetic changes occur in melanoma. These modifications include in particular aberrant DNA methylation of cytosine (5-methylcytosine (5mC)) at CpG sites - including both hyper- and hypomethylation-, loss of 5-hydroxymethylcytosine (5hmC), histone modifications and ncRNA expression [4–6]. Several studies have associated DNA methylation changes with melanoma initiation and progression [7–

[10] and genome-wide analysis correlated DNA methylation signatures and silenced genes to different melanoma stages [11–19]. We have previously provided evidence supporting that aberrant DNA methylation regulates genes involved in melanoma progression and aggressiveness by identifying a microRNA, miR-199a-3p, regulated by DNA methylation and whose up-regulation led to reduced tumor cell invasion *in vitro* and *in vivo* [20]. Next, we used a multi-step strategy to identify the aberrant DNA methylation patterns that characterize human melanoma aggressiveness independently of the physiological background [21]. Among the aberrant methylated CpGs pattern that mark melanoma aggressiveness in patient primary tumors, we found the *PCDHB15* gene. This gene belongs to a cluster encoding for adhesion molecules, the protocadherins, related to the cadherin superfamily. Some protocadherins are predominantly expressed within the central nervous system during development, suggesting important neurobiological roles. Others, expressed in tissues at adult stages, seem to regulate cellular differentiation, tissue regeneration and maintenance. Interestingly, while their functional role remains mostly elusive, loss of protocadherins has been linked to several cancer types [22]. In particular, a region of 800kb, which includes protocadherins α and γ families, was reported to display long-range epigenetic silencing (LRES) in breast cancer [23], Wilm's tumor [24] and colorectal cancer [25]. In neuroblastoma, aberrant DNA methylation of the *PCDHB* family was proposed as part of the CpG island methylator phenotype (CIMP) [26] and was strongly associated with poor prognosis [27–29].

Here, we show that *PCDHB15,* a member of this cluster of genes, marks melanoma aggressiveness and plays a functional role in regulating hallmarks of cancerogenesis. We observed that *PCDHB15* is hypermethylated at the 5' end of its unique exon and is not expressed in two metastatic melanoma-derived cell lines, WM266-4 and WM983A. TCGA data confirm that *PCDHB15* hypermethylation is observed in patient metastasis samples compared to primary tumor samples. Interestingly, the expression of this gene was modulated upon

treatment with the DNA demethylating agent 5-aza-deoxycytidine (5azadC). In addition, over-expression of *PCDHB15* impaired metastatic melanoma cell invasiveness and aggregation *in vitro*, and metastasis formation *in vivo*. For the first time, our findings support a potential role of *PCDHB15* silencing contributing to melanoma aggressiveness by important DNA methylation modifications of the gene.

Material and methods

Cell Culture

The WM115 and WM266-4 cells, as well as WM983A and WM983B cells, were established from a primary VGP melanoma and a metastasis from a same patient, respectively[30]. *In vitro*, the cell lines with metastatic origin (WM266-4, WM983B) displayed a higher invasive potency, compared to cells from primary melanomas (WM115, WM983A), as assessed in 3D spheroids invasion assays[31] and human reconstructed skin models [32–34].

The WM266-4 and WM115 cells (obtained from the American Type Culture Collection) were grown in DMEM (Invitrogen, France) supplemented with 10% fetal bovine serum (Sigma, France), 2 mM glutamine, 100 UI/mL penicillin-streptomycin, and in a 5% CO2 atmosphere. The WM983A and WM983B cells (purchased from the Coriell Institute) were grown in MCDB153 medium with 20% Leibovitz L-15 medium (v/v), 2% FBS heat-inactivated (v/v), 5 µg/mL insulin and 1.68 mM CaCl2. The numerations of viable cells were performed using an Automated Cell Viability Analyzer (Beckman Coulter Vi-Cell).

Establishment of stable cell lines

WM266-4 cells were seeded at $6x10^5$ cells in 60 mm dishes and transfected 24h later using Lipofectamine 2000 (Invitrogen) with 1 µg of the pCMV6-*PCDHB15* plasmid (DDK-tagged

PCDHB15, RC207719, Clinisciences) or the pCMV6-MOCK plasmid corresponding to the same plasmid without the *PCDHB15* cDNA sequence (obtained from the pCMV6-*PCDHB15* plasmid by digestion with by EcoRI and XhoI, and self-ligation with a linker). The selection of transfected cells was performed in a medium containing 0.8 mg/mL of geneticin (Gibco). Cell lines expressing *PCDHB15* were established from 3 of 15 isolated clones. PCDHB15 expression was characterized by RT-qPCR . The control cell line (WM266-4 MOCK) is a pool of transfected cells with the pCMV6-MOCK plasmid. Transfected cells were maintained in culture in a medium containing 0.6 mg/mL geneticin for 10 passages. These modifications did not impact morphology proliferation and viability. All experiments were conducted under 20 cell passages in culture.

Tumor samples

Tumor samples from four melanoma patients were retrieved from the tumor tissue bank at the Department of Pathology, IUCT-O Toulouse Hospital (France). The study was carried out in accordance with the institutional review board-approved protocols (CRB, AC-2013-1955), and the procedures followed the Helsinki Declaration. Pathological specimens consisted of frozen samples from primary (n=13) and metastasis samples (n=9). Additional frozen primary melanoma samples ($n=5$) were provided by the Department of Experimental Oncology, European Institute of Oncology, Milan (Italy).

Cells treatment with 5-aza-*2'*-deoxycytidine (5azadC)

5-aza-2'-deoxycytidine (5azadC, decitabine) was bought from Sigma-Aldrich (France) and dissolved in acidic water at 10mM and stored in single-use aliquots at -20°C.

WM-266-4 cells were seeded at the density of 6 $x10^6$ cells per 75 cm^2 flasks (day 0) and treated with 5azadC after a 12 h period to allow cell attachment and synchronization in G0/G1 phase.

Cells were treated daily for 72h (day 1, 2, 3) at the indicated concentration of 5azadC. They were collected at day 4 for analysis of DNA methylation patterns by pyrosequencing and day 7 for expression analyses.

Genomic DNA isolation

Genomic DNA from cell lines was isolated using the DNeasy Tissue kit (Qiagen, France). Genomic DNA from patients' samples was isolated using the QiaAmp kit (Qiagen, France).

`

Bisulfite pyrosequencing

Quantitative DNA methylation analysis was performed by pyrosequencing of bisulfite-treated DNA as previously described [35]. Sequences including CpGs were amplified using 20 ng of bisulfite-treated human genomic DNA and 5–7.5 pmol of forward and reverse primer, one being biotinylated. Two pairs of PCR primers were designed for PCR1 (CpG 1, 2, 3 and 4) and PCR2 (CpG 5 and 6) (Figure 1A). PCR were designed around the hypermethylated probes from previous Illumination 450k Bead Chip analysis [21].

PCR1: Biotin-TTTAGAGTTGGTGTTGGATATAGAA (Forward) and CCAAAACCAAAATAAAAATCTAAAC (Reverse);

PCR2: TTTAGATTTTTATTTTGGTTTTGGA (Forward) and Biotin-TATAATATCTCTCCATTTATCCCAATATCT (Reverse).

Reaction conditions were 1 × HotStar® Taq buffer (Qiagen) supplemented with 1.6 mM $MgCl_2$, 100 μM dNTPs and 2.0 U HotStar Taq polymerase (Qiagen) in a 25 μL volume. The PCR program consisted of a denaturing step of 15 min at 95°C, followed by 50 cycles of 30 s at 95°C, 30 s at 60°C and 20 s at 72°C, with a final extension of 5 min at 72°C. A total of 10 μL of PCR product was rendered single-stranded as previously described and 4 pmol of the respective sequencing primers were used for analysis. Quantitative DNA methylation analysis

was carried out on a PSQ 96MD system with the PyroGold SQA Reagent Kit (Qiagen) and results were analyzed using the PyroMark software (V.1.0, Qiagen).

TCGA DNA methylation data analysis

The TCGA-SKCM DNA methylation data was downloaded from GDAC Firehose Broad [36] on February 2021. Normalized beta values for the Illumina probes nearby the *PCDHB15* gene were selected for comparative analyses. DNA methylation for primary melanoma (PRM), lymph node metastasis (LNM), and distant organ metastasis (DOM) was summarized using the mean value and the standard error of the mean. Differential DNA methylation was assessed by the Wilcoxon Rank-Sum test in R. All p-values from multiple comparisons (>50 tests) were corrected using the False discovery rate (FDR) method. The R/ggplot2 package was used for data visualization.

mRNA quantification

RNA was purified using the RNeasy Mini Kit (Qiagen, France) and quantified on a NanoDrop2000 (ThermoScientific).

Quantification of *PCDHB15* mRNA was performed by RT-qPCR. Total RNA (2 µg) was reverse transcribed into cDNA with the iScript cDNA Synthesis Kit (BioRad, USA). Real-time PCR was performed according to the manufacturer's recommendations, using SsoAdvanced™ SYBR® Green supermix (Bio-Rad). The primers were: AGCAGGCCGAGCTCAGATTA (forward) and ATTGGCGTCCAAGACCAAGA (reverse). A CFX384 Touch™ Real-Time PCR Detection System from Biorad (Marnes-la-Coquette, France) was used to run the following PCR program: 95°C 10 min followed by 40 cycles of 15 sec at 95°C, 30 sec at 65°C for elongation, ended with a fusion cycle to determine the Tm of each amplification product.

The PCR data were analyzed with the CFX Manager v3.0 software (Biorad) to generate the Ct values. The following quality controls were applied: amplification of a single product, no amplification in the NRT (No reverse transcription) condition, efficiency close to 100%, $R^2 >$ 0.98 and SD between technical triplicates <0.3. The $2-\Delta\Delta Ct$ method was used to generate the gene expression ratios by amplification of TBP (TATA box binding protein) TTGACCTAAAGACCATTGCACTTCGT (Forward) and TTACCGCAGCAAACCGCTTG (reverse) as normalizing control and data were presented as mRNA fold change of target RNA.

Western-blot analysis

Total protein extract was obtained from confluent cells grown in 75 cm^2 flasks. The cells were lysed in protein extraction buffer (10mM Tris HCl, 120mM NaCl, 1% NP40, 1mM EDTA, 1mM DTT and 1X proteases inhibitor (Complete™, EDTA-free Protease Inhibitor Cocktail, Sigma Aldrich)). Samples were separated on 10% SDS-PAGE gels and transferred onto polyvinylidene difluoride membranes. After saturation with 5% dry milk in Tris NaCl 1% Tween 20, membranes were incubated with either anti-PCDHB15 antibody (NBP1-87322, Novus Biologicals), anti-DDK antibody (4C5, TA50011, Origene) (1/1000 diluted in 5% dry milk in Tris NaCl 1% Tween 20) or anti-β actin antibody (MAB1501, Millipore, 1/1000 in 5% dry milk). After washes, the membranes were revealed with secondary HRP-coupled antibodies (Sigma Aldrich). The signals were detected by ECL for β-actin (GE Healthcare) and Immobilon Western HRP Substrate (Millipore) for PCDHB15 and DDK. The chemoluminescent signals were acquired with a G:box imaging system (Syngene).

PCDHB15 cell surface expression

The expression of PCDHB15 at the cell surface was analyzed by flow cytometry. Cells were detached with 2 mM EDTA in PBS and incubated for 45 min at 4°C with 1µg/mL of anti-

PCDHB15 antibody (NBP1-87322, Novus Biologicals) in PBS supplemented with 1% BSA. Cells were washed, counterstained with Alexa-647-conjugated goat anti-rabbit Ig antibodies (Invitrogen) and incubated with 0.5 mg/mL DAPI (Sigma). PCDHB15 expression was monitored on live cells (gated as DAPI-negative cells) on a LSRII flow cytometer using the Diva software (both from BD Biosciences, Le Pont-De-Claix, France).

3D cell invasion assay

WM-266-4 cells were seeded in 96-well plates coated with agarose 1% (Sigma-Aldrich) in PBS (3000 cells in 100 µL medium per well). After 2 days at 37°C in a 5% CO_2 atmosphere, cells from one spheroid with a diameter of approximately 300 µm. For each condition, six spheroids were individually embedded in EMEM media (Lonza) containing 1% of bovin collagen I (BD Biosciences) and 2% SVF. Bright field images from the initial spheroids were acquired with an Axiovert 200M device (5X Plan-Neofluor objective, Carl Zeiss, Germany). After 24h at 37°C, spheroids were labelled 1h with 2.5 µM calcein (calcein AM, BD Pharmingen) in PBS and fluorescent 6 z-stack images with 20 µm intervals were acquired. The fluorescent pictures were stacked and the total sizes of the spheroids were measured using the Image J (NIH) software. Invasion areas were obtained by subtracting the initial size of the spheroid. The invasion index represents the invasion area at 24h normalized to the initial spheroid area. If cytotoxic effects appear, the initial spheroid area decrease and the data are not considered.

Aggregation assay

Cells were dissociated with 2mM EDTA in PBS and seeded in a CELLSTAR® Cell-Repellent surface 96-well plate (Greiner Bio-One) (500 cells in 100µL medium per well), then centrifuged at 200*g* for 8 min and left at rest for 45 min before time-lapse experiments. Time-lapse video microscopy images were acquired over 20h (1 acquisition/15min), by using an inverted

widefield Zeiss Axio Observer Z1 microscope fitted with a 0.3 N.A 10x objective and a CoolSNAP CDD camera (Roper scientific). At each time point and position, 5-µm spaced z-stacks in brightfield were acquired using the Meta-Morph software. At each time point, and for each aggregate, areas of the cell aggregates were quantified using an algorithm developed on MATLAB software [37]. The aggregate areas were normalized to the calculated area at the beginning of time-lapse microscopy.

In vivo metastasis experiments

The animals were handled and cared for in accordance with the Guide for the Care and Use of Laboratory Animals (National Research Council, 1996) and European Directive EEC/86/609, under the supervision of the authorized investigators. Un-anesthetized 7-week-old female SCID mice (ENVIGO RMS SARL, Gannat, France) were injected into the tail vein with 3×10^6 viable cells in 200-µL PBS (WM266-4 WT, WM266-4-pCMV mock or each stable clone overexpressing the *PCDHB15* gene). Groups were constituted of n=15 animals for injection with mock, clone 8 and clone 12; n=14 for clone 13. Twenty-one days after injection, mice were dissected and the organs (except brain) were visually inspected. Lungs only presented detectable metastases. They were recovered, formalin-fixed and paraffin-embedded. Sections were stained with hematoxylin and eosin (H&E). The number and area of metastasis were measured in whole lung sections by immunostaining with Tyrosinase antibody Mob299–05 (1/500) (Diagnostic BioSystem, Pleasanton, CA-USA). 3DHistech (Panoramic 250) was used to scan sections and measure metastases area. Statistics were performed using the Mann-Whitney test.

Results

PCDHB15 is hypermethylated in aggressive melanoma cells and patient samples.

By comparing the DNA methylation profile of three highly aggressive metastatic melanoma cell lines (WM-266-4, M4BeS2 and TW12) to their less-aggressive counterpart derived from the same patient (WM115 and M4Be, respectively) by genome-wide DNA methylation analysis (BeadChip Illumina 450K, deposited as GSE155856), we identified hypermethylated genes

located in gene clusters [21]. Among them, we focused our analysis on *PCDHB15*, which belongs to the protocadherin beta family cluster located on chromosome 5 (5q31.3). In WM115 and WM266-4 cells which are derived, respectively, from the primary tumor and the cutaneous metastasis of the same patient, *PCDHB15* showed differential methylation above 40% in at least two CpGs positions located at +566 and +610 pb from the TSS, respectively (Figure 1A). The differential methylation status in this region was confirmed by pyrosequencing after bisulfite conversion and PCR amplification of six close CpGs, in WM115 and WM266 cells, as well as in the cell line pair WM983A and WM983B derived from the same patient but with different aggressiveness status (Figure 1B). The boxplots indicate that the DNA methylation median for *PCDHB15* in this region was higher in WM266-4 and WM983B (metastatic) cells compared to WM115 and WM983A (primary) cells, respectively. Interestingly, higher DNA methylation levels were also found in nine patient metastasis samples compared to 18 primary melanoma samples (Figure 1C). We also investigated the DNA methylation of this gene in The Cancer Genome Atlas database (Figure 1D), showing a statistically non-significant increase in DNA methylation in lymph node (LNM) and distant organ metastasis (DOM) compared to primary melanomas (PRM). Furthermore, a CpG (probe cg24941075) located close to the PCDHB15 promoter region in a transcription factor region (CTCF) was found to be hypermethylated in several DOM patients, leading to a significant difference between DOM *versus* PRM and LNM groups (Figure 1D).

DNA hypermethylation of *PCDHB15* is associated with decreased gene expression that is reversed upon 5azadC treatment.

We then investigated whether the DNA hypermethylation of *PCDHB15* gene 5'-end was associated with gene silencing. The methylation status and expression in WM115 *versus* WM266-4 cells were inversely correlated: WM115 cells, in which *PCDHB15* 5'-end was less methylated than in WM266-4 cells, expressed a two-fold higher amount of *PCDHB15* mRNA (Figure 1E). Treatment of WM266-4 cells with increasing concentrations of the DNA demethylating agent 5azadC for 3 days induced a decrease in DNA methylation of *PCDHB15* in a dose-dependent manner with a plateau at 55% (Figure 1E). Concomitantly, its expression increased significantly upon treatment with 0.1 µM to 0.32µM of 5azadC, resulting in a 2-fold increase compared to the level observed in WM115 cells (Figure 1F).

These results indicated a potential role for DNA methylation in the silencing of *PCDHB15* correlating with the aggressiveness of metastatic melanoma. We next investigated this hypothesis.

***PCDHB15* overexpression impairs melanoma cells 3D aggregation.**

PCDHB15 was overexpressed with a C-terminal DDK-tagged construct in the metastatic WM266-4 cells, in which *PCDHB15* is silenced (Figure 2A). Three clones overexpressing *PCDHB15* were selected and characterized (clone 8, 12 and 13, figure 2B). All three clones produced high levels of *PCDHB15* mRNA compared to mock-transfected and wild type WM266-4 cells (Figure 2C), but displayed different content of the full-length protein (Figure 2B). In addition, a significant amount of protein was detected at the cell surface by cell surface labeling with an anti-PCDHB15 antibody directed against the N-terminal portion of the protein and flow cytometry measurement (Figure 2D).

Next, we studied the effect of the overexpression of *PCDHB15* on the aggregation of melanoma cells by monitoring the spontaneous formation of spheroids in the metastatic WM266-4 cell line and the three clones. The size and kinetics of the formation of the spheroids were studied by brightfield video-microscopy. As early as 2 hours after seeding, WM266-4 cells gathered and formed round aggregates with cell-to-cell interaction that strengthened with time (Figure 3A). In contrast, cells overexpressing *PCDHB15* formed loose aggregates with different kinetics and maintained irregular shapes over time, suggesting a reluctance to engage straight contacts (figure 3A and B).

***PCDHB15* overexpression impairs melanoma cells 3D invasion.**

Another feature of the metastatic WM266-4 cell line is its 3D invasion ability, as we demonstrated previously [20]. After 72h of culture in non-adherent conditions, WM266-4 cells

spontaneously formed spheroids that were included in a collagen matrix (figure 4A). Invasion in the collagen matrix was measured after 24h (figure 4B). Noteworthy, WM115 cells formed highly cohesive spheroids, but had no invasion capacity under these conditions. After collagen inclusion, the overexpression of *PCDHB15* had little effect on the spheroid size (figure 4C), but significantly reduced the invasive properties of WM266-4 cells (figure 4D). Interestingly, the greatest effect was observed with the two cell lines (#8 and #12) producing intermediate protein levels.

***PCDHB15* overexpression impairs lung metastasis formation in mice.**

The inhibitory effect of *PCDHB15* overexpression on *in vitro* melanoma cell aggregation and invasion led us to investigate the capacity of *PCDHB15* expressing melanoma cells to form lung metastasis in mice after intravenous injection as does the metastatic WM266-4 cell line [20]. We compared the effect of the three WM266-4 clones overexpressing *PCDHB15* to cells stably transfected with a void construct (mock cells). Immunohistochemical analysis of lungs 21 days after injection showed a dramatic decrease in lung metastasis formation with cells overexpressing *PCDHB15* compared to mock control WM266-4 cells (figure 5A). This result was confirmed by statistical analysis of the number (Figure 5B) and size (Figure 5C) of metastases, showing that the overexpression of *PCDHB15* reduces *in vivo* the invasion capacities of metastatic melanoma cells.

Discussion

Melanoma generally evolves in a stepwise manner from initial benign or dysplastic *naevi* to metastatic melanoma, via two intermediate phases, the radial (RGP) and the vertical growth (VGP) phases [38,39]. To characterize the extent and nature of DNA methylation modifications through melanoma progression, we have compared the DNA methylation profiles of melanoma

cell lines representative of different aggressiveness status and focused our interest on genes that were hypermethylated in the most aggressive cell lines. This revealed the role of DNA methylation in the regulation of the mir199-A2 which down-regulation confers invasive traits in melanoma [20]. More recently, by comparing the genomic repartition of DNA methylation in cell lines of different aggressiveness status, we identified clusters of DNA hypermethylation that characterizes melanoma aggressiveness and, in particular, the gene *PCDHB15* [21]. *PCDHB15* belongs to the protocadherin β gene cluster located on chromosome 5q31. The clustered protocadherins α, β, and γ were mostly studied as putative neural receptors [40–42] that mediate the synaptic adhesive code between neurons in synaptogenesis. Stochastic single-neuron expression of clustered protocadherin protein isoforms by a mechanism involving alternative promoter choice [43] generated distinct cell-surface identities [44,45]. In the human central nervous system, the expression patterns of the PCDH-β genes are similar to those of the PCDH-α and PCDH-γ genes and contain 16 genes and 3 pseudogenes [42]. Each sequence corresponds to a single variable region exon encoding an extracellular domain with six characteristic cadherin ectodomain repeats (EC1-6), a transmembrane domain and an intracellular domain. All three types of protocadherins -α, -β, -γ can engage in isoform-specific trans-homophilic interactions [46]. They mediate neural self-recognition and non self-discrimination. Interestingly, although classified as adhesion molecules, protocadherin homophilic interactions trigger neurite self-avoidance [47] that prevents interactions of axons and dendrites from the same neuron during development. However, the functional role of *PCDH* genes in tissues other than the brain is poorly explored. Several reports in the literature pointed towards a potential role of protocadherins as tumor suppressors in several cancers [48]. Considering that neurons and melanocytes are derived from the same embryonic tissue, these findings prompted us to characterize the functional role of PCDHB15 in cutaneous melanoma cells.

We showed that *PCDHB15* is strongly DNA hypermethylated at the 5'end of its single exon, in the most aggressive melanoma cell lines compared to the less aggressive ones, as well as in the metastases compared to the corresponding primary melanomas. In cell lines, DNA hypermethylation of *PCDHB15* was associated with lower expression, which was reversed upon treatment with the demethylating drug 5azadC. Of note, the demethylation by 5azadC reached a plateau at 55%, probably meaning that all the accessible cytosines in the DNA sequence were replaced by 5azadC. Interestingly, a negative correlation between PCDHB15 promoter methylation and PCDHB15 expression was also reported in breast cancer[49]. Nevertheless, whereas these data strongly pointed out the role of DNA methylation in the regulation of *PCDHB15* expression, the direct involvement of the methylation in the regulatory regions at the 5'end of the gene remains to be confirmed. To study the correlation, several approaches can be uses as a CpG-free luciferase reporter vector system [50] or CRISPR/Cas9-mediated epigenetic edition[51]. Here, we evaluated whether the treatment with the demethylation agent, 5azadC, at low doses reverts *PCDHB15* silencing, as we have shown that 5azadC treatment at low doses reverted melanoma cell invasion in 3D-invasion assays and *in vivo* metastasis formation [20]. We observed that *PCDHB15* expression was up-regulated by 5azadC treatment, in support of a regulatory role of DNA methylation at its promoter.

The stable overexpression of *PCDHB15* in cells, in which *PCDHB15* is silenced by DNA hypermethylation, dramatically impaired their aggregation capacity suggesting a non-adhesive role for PCDHB15 in agreement with a self-avoidance process as described for neurons [47]. Protocadherins β harbor extracellular cadherin motifs able to interact homophilically in trans, but how their truncated intracytoplasmic domain translate in the alteration of cellular adhesion remains to be understood [22]. Lower aggregation upon *PCDHB15* overexpression is associated with impaired 3D invasiveness, suggesting the potential importance of an aggregative behavior in the invasive abilities of melanoma cells. This is in agreement with the reported lower cancer

cell dissemination when tumor cells migrate as individual cells compared to aggregated cells [52]. Taken together, these *in vitro* effects suggest that silencing of *PCDHB15* in melanoma cells participates in the fine-tuning of the aggregative behavior of melanoma cells during melanoma progression and favors specific metastatic properties. The *in vivo* experiment confirmed the *in vitro* findings, showing that the overexpression of *PCDHB15* impairs the formation of lung metastases in mice. Of note, whereas the three *PCDHB15*-expressing cell lines showed similar tendencies in the different functional assays, they did not highlight a strict correlation between the levels of PCDHB15 expression and their inhibitory effects, compared to the parental cell line. One cannot exclude that high expression levels of the protein could alter its proper processing as well as its cellular function. Nevertheless, the obtained data parallel what has been observed in breast cancer cell lines, in which overexpression of other members of the PCDH-β gene family (*PCDHB4* and *PCDHB19)* inhibited anchorage-independent cell growth in soft agar, colony formation ability and *in vivo* tumor growth in NOD/SCID mice [53].

In concordance with our findings, *PCDHB15* was identified as a part of a specific methylation signature across breast and colon cancer [54], as *PCDHB13* in Non-Small Cell Lung Cancer[55]. A functional role for the hypermethylation and gene silencing of PCDHαβγ family genes (*PCDHAC2*, *PCDHB7*, *PCDHB15*, *PCDHGA1*, and *PCDHGA6*) was also identified recently in colorectal cancer influencing the WNT/B-catenin pathway implicated in proliferation, survival and migration[56]. More recently, *PCDHB15* was proposed has a potential tumor suppressor in breast cancer, based on the observation of a positive correlation between PCDHB15 expression and relapse-free survival [49]. Interestingly, ectopic expression of *PCDHB15*, which is down-regulated by DNA methylation in the MDA-MB-231 breast cell line, suppressed colony formation.

Conclusions

In this study, we demonstrate an epigenetic regulation of the expression of the *PCDHB15* gene in melanoma cell lines. This gene is silenced in metastatic cells and its stable overexpression reduced cell aggregation and invasion capacity *in vitro* and *in vivo*. Taken together, our data suggest for the first time a potential role of tumor suppressor for *PCDHB15* in melanoma. Mechanisms by which PCDHB15 may play a role in aggregation and invasion are to be further studied. In accordance with findings in other cancers, we propose that the role of the protocadherin genes and their interactions in cancer progression will be an area of interest to investigate in the future.

ACKNOWLEDGEMENTS

The authors thank the Instituto de la Salud Carlos III and the Asociación Española Contra el Cancer (AECC) Foundation Junta Balear for supporting D.M.M. and M.E.

LIST OF ABBREVIATIONS

5azadC: 5aza-2′-deoxycytidine
AJCC: American joint committee on cancer
CIMP: CpG island methylator phenotype
CpG: Cytosine preceding guanine nucleotide dimer 5'-3'direction
DNA: deoxyribonucleic acid
DOM: Distant organ metastasis
LNM: lymph node metastasis
ncRNA: non-coding ribonucleic acid
PBS: phosphate buffer saline
PCDHB: protocadherin beta
PRM: Primary tumor

DECLARATIONS

Ethical Approval
Not applicable

Competing interests
The authors declare no competing intersts

Authors' contributions
A.C. run the experiments, analysed the data, drafted the work. C.D., acquired and analysed data, revised the manuscript. V.L. and L.R. developed the in vitro aggregation assays and acquired data. M.E. and D.M.M. performed the TCGA analysis. L.Lamant and L.Lanfrancone chose and prepared the DNA patient samples. A.P. and G.F. proposed and prepared the cellular and in vivo models. F.B. and J.T. acquired and analysed bisulfite pyrosequencing data. C.E., J.R. and P.B.A. designed the study acquired and analysed data, supervised the study, acquired funds and drafted the manuscript.

Funding
This work was supported to P.B.A. by Centre National de la Recherche Scientifique (CNRS) [ATIP], Région Midi Pyrenées [Equipe d'Excellence and FEDER CNRS/Région Midi Pyrenées], Fondation InNaBioSanté and by the National Research Agency (ANR: Agence Nationale de la Recherche) "Investissement d'avenir" [ANR-11-PHUC-001, CAPTOR research program].

Availability of data and materials
Not applicable

REFERENCES

1. Ferlay, J. *et al.* Cancer incidence and mortality worldwide: sources, methods and major patterns in GLOBOCAN 2012. *International journal of cancer* **136**, E359-86 (2015).
2. Teterycz P, Ługowska I, Koseła-Paterczyk H & Rutkowski P. Comparison of seventh and eighth edition of AJCC staging system in melanomas at locoregional stage. *World J Surg Oncol.* **17**, 129 (2019).
3. Rebecca VW, Somasundaram R & Herlyn M. Pre-clinical modeling of cutaneous melanoma. *Nat Commun.* **11**, 2858 (2020).
4. Baylin, S. B. & Jones, P. A. Epigenetic Determinants of Cancer. *Cold Spring Harb Perspect Biol* **8**, (2016).
5. Ortiz-Barahona, V., Joshi, R. S. & Esteller, M. Use of DNA methylation profiling in translational oncology. *Seminars in Cancer Biology* S1044579X20302716 (2020) doi:10.1016/j.semcancer.2020.12.011.

6. Sarkar, D., Leung, E. Y., Baguley, B. C., Finlay, G. J. & Askarian-Amiri, M. E. Epigenetic regulation in human melanoma: past and future. *Epigenetics* **10**, 103–21 (2015).
7. Howell, P. M., Jr. *et al.* Epigenetics in human melanoma. *Cancer control : journal of the Moffitt Cancer Center* **16**, 200–18 (2009).
8. Martinez-Cardus, A., Vizoso, M., Moran, S. & Manzano, J. L. Epigenetic mechanisms involved in melanoma pathogenesis and chemoresistance. *Annals of translational medicine* **3**, 209 (2015).
9. Schinke, C. *et al.* Aberrant DNA methylation in malignant melanoma. *Melanoma research* **20**, 253–65 (2010).
10. Sigalotti, L. *et al.* Epigenetics of human cutaneous melanoma: setting the stage for new therapeutic strategies. *Journal of translational medicine* **8**, 56 (2010).
11. Bonazzi, V. F. *et al.* Cross-platform array screening identifies COL1A2, THBS1, TNFRSF10D and UCHL1 as genes frequently silenced by methylation in melanoma. *PloS one* **6**, e26121 (2011).
12. Conway, K. *et al.* DNA-methylation profiling distinguishes malignant melanomas from benign nevi. *Pigment cell & melanoma research* **24**, 352–60 (2011).
13. Gao, L. *et al.* Promoter CpG island hypermethylation in dysplastic nevus and melanoma: CLDN11 as an epigenetic biomarker for malignancy. *The Journal of investigative dermatology* **134**, 2957–66 (2014).
14. Gao, L. *et al.* Genome-wide promoter methylation analysis identifies epigenetic silencing of MAPK13 in primary cutaneous melanoma. *Pigment cell & melanoma research* **26**, 542–54 (2013).
15. Koga, Y. *et al.* Genome-wide screen of promoter methylation identifies novel markers in melanoma. *Genome research* **19**, 1462–70 (2009).

16. Lauss, M. *et al.* DNA methylation subgroups in melanoma are associated with proliferative and immunological processes. *BMC medical genomics* **8**, 73 (2015).
17. Marzese, D. M., Huynh, J. L., Kawas, N. P. & Hoon, D. S. Multi-platform Genome-wide Analysis of Melanoma Progression to Brain Metastasis. *Genomics data* **2**, 150–152 (2014).
18. Sigalotti, L. *et al.* Whole genome methylation profiles as independent markers of survival in stage IIIC melanoma patients. *Journal of translational medicine* **10**, 185 (2012).
19. Vizoso, M. *et al.* Epigenetic activation of a cryptic TBC1D16 transcript enhances melanoma progression by targeting EGFR. *Nature medicine* **21**, 741–50 (2015).
20. Desjobert, C. *et al.* Demethylation by low-dose 5-aza-2′-deoxycytidine impairs 3D melanoma invasion partially through miR-199a-3p expression revealing the role of this miR in melanoma. *Clin Epigenet* **11**, 9 (2019).
21. Carrier, A. *et al.* DNA Methylome Combined with Chromosome Cluster-Oriented Analysis Provides an Early Signature for Cutaneous Melanoma Aggressiveness. *BioRxiv* (2022) doi:10.1101/2022.04.11.487909.
22. Pancho, A., Aerts, T., Mitsogiannis, M. D. & Seuntjens, E. Protocadherins at the Crossroad of Signaling Pathways. *Front Mol Neurosci* **13**, 117 (2020).
23. Shan, M. *et al.* Aberrant expression and functions of protocadherins in human malignant tumors. *Tumor Biol.* **37**, 12969–12981 (2016).
24. Novak, P. *et al.* Agglomerative epigenetic aberrations are a common event in human breast cancer. *Cancer research* **68**, 8616–25 (2008).
25. Dallosso, A. R. *et al.* Frequent long-range epigenetic silencing of protocadherin gene clusters on chromosome 5q31 in Wilms' tumor. *PLoS genetics* **5**, e1000745 (2009).

26. Dallosso, A. R. *et al.* Long-range epigenetic silencing of chromosome 5q31 protocadherins is involved in early and late stages of colorectal tumorigenesis through modulation of oncogenic pathways. *Oncogene* **31**, 4409–19 (2012).
27. Abe, M. *et al.* CpG island methylator phenotype is a strong determinant of poor prognosis in neuroblastomas. *Cancer research* **65**, 828–34 (2005).
28. Asada, K., Abe, M. & Ushijima, T. Clinical application of the CpG island methylator phenotype to prognostic diagnosis in neuroblastomas. *Journal of human genetics* **58**, 428–33 (2013).
29. Hughes, L. A. *et al.* The CpG island methylator phenotype: what's in a name? *Cancer research* **73**, 5858–68 (2013).
30. Hsu, M.-Y., Elder, D. E. & Herlyn, M. Melanoma: The Wistar Melanoma (WM) Cell Lines. in *Human Cell Culture* (eds. Masters, J. R. W. & Palsson, B.) vol. 1 259–274 (Kluwer Academic Publishers, 2002).
31. Luca, A. D. *et al.* The nitrobenzoxadiazole derivative MC3181 blocks melanoma invasion and metastasis. *Oncotarget* **8**, 15520–15538 (2017).
32. Vörsmann, H. *et al.* Development of a human three-dimensional organotypic skin-melanoma spheroid model for in vitro drug testing. *Cell Death Dis* **4**, e719–e719 (2013).
33. Saltari, A. *et al.* CD271 Down-Regulation Promotes Melanoma Progression and Invasion in Three-Dimensional Models and in Zebrafish. *Journal of Investigative Dermatology* **136**, 2049–2058 (2016).
34. Bourland, J., Fradette, J. & Auger, F. A. Tissue-engineered 3D melanoma model with blood and lymphatic capillaries for drug development. *Sci Rep* **8**, 13191 (2018).
35. Tost, J. & Gut, I. G. DNA methylation analysis by pyrosequencing. *Nature protocols* **2**, 2265–75 (2007).

36. Akbani, R. *et al.* Genomic Classification of Cutaneous Melanoma. *Cell* **161**, 1681–1696 (2015).
37. Saias, L., Gomes, A., Cazales, M., Ducommun, B. & Lobjois, V. Cell-Cell Adhesion and Cytoskeleton Tension Oppose Each Other in Regulating Tumor Cell Aggregation. *Cancer Res* **75**, 2426–2433 (2015).
38. Miller, A. J. & Mihm, M. C., Jr. Melanoma. *The New England journal of medicine* **355**, 51–65 (2006).
39. Zaidi, M. R., Day, C. P. & Merlino, G. From UVs to metastases: modeling melanoma initiation and progression in the mouse. *The Journal of investigative dermatology* **128**, 2381–91 (2008).
40. Kohmura, N. *et al.* Diversity revealed by a novel family of cadherins expressed in neurons at a synaptic complex. *Neuron* **20**, 1137–51 (1998).
41. Shapiro, L. & Colman, D. R. The diversity of cadherins and implications for a synaptic adhesive code in the CNS. *Neuron* **23**, 427–30 (1999).
42. Wu, Q. & Maniatis, T. A striking organization of a large family of human neural cadherin-like cell adhesion genes. *Cell* **97**, 779–90 (1999).
43. Tasic, B. *et al.* Promoter choice determines splice site selection in protocadherin alpha and gamma pre-mRNA splicing. *Molecular cell* **10**, 21–33 (2002).
44. Hirano, K. *et al.* Single-neuron diversity generated by Protocadherin-beta cluster in mouse central and peripheral nervous systems. *Frontiers in molecular neuroscience* **5**, 90 (2012).
45. Junghans, D. *et al.* Postsynaptic and differential localization to neuronal subtypes of protocadherin beta16 in the mammalian central nervous system. *The European journal of neuroscience* **27**, 559–71 (2008).

46. Schmitt, C. J. *et al.* Homo- and heterotypic cell contacts in malignant melanoma cells and desmoglein 2 as a novel solitary surface glycoprotein. *The Journal of investigative dermatology* **127**, 2191–206 (2007).
47. Thu, C. A. *et al.* Single-cell identity generated by combinatorial homophilic interactions between alpha, beta, and gamma protocadherins. *Cell* **158**, 1045–59 (2014).
48. Zipursky, S. L. & Sanes, J. R. Chemoaffinity revisited: dscams, protocadherins, and neural circuit assembly. *Cell* **143**, 343–53 (2010).
49. Chiang, C.-C. *et al.* PCDHB15 as a potential tumor suppressor and epigenetic biomarker for breast cancer. *Oncol Lett* **23**, 117 (2022).
50. Klug, M. & Rehli, M. Functional Analysis of Promoter CPG-Methylation using a CpG-Free Luciferase Reporter Vector. *Epigenetics* **1**, 127–130 (2006).
51. Kang, J. G., Park, J. S., Ko, J.-H. & Kim, Y.-S. Regulation of gene expression by altered promoter methylation using a CRISPR/Cas9-mediated epigenetic editing system. *Sci Rep* **9**, 11960 (2019).
52. Aceto, N. *et al.* Circulating tumor cell clusters are oligoclonal precursors of breast cancer metastasis. *Cell* **158**, 1110–22 (2014).
53. Guo, H. *et al.* Transcriptional regulation of the protocadherin beta cluster during Her-2 protein-induced mammary tumorigenesis results from altered N-glycan branching. *The Journal of biological chemistry* **287**, 24941–54 (2012).
54. Zhang, C. *et al.* The Identification of Specific Methylation Patterns across Different Cancers. *PloS one* **10**, e0120361 (2015).
55. Ting, C.-H. *et al.* FOSB^{-}PCDHB13 Axis Disrupts the Microtubule Network in Non-Small Cell Lung Cancer. *Cancers (Basel)* **11**, (2019).

56. Wong, C. C. *et al.* In Colorectal Cancer Cells With Mutant KRAS, SLC25A22-Mediated Glutaminolysis Reduces DNA Demethylation to Increase WNT Signaling, Stemness, and Drug Resistance. *Gastroenterology* (2020) doi:10.1053/j.gastro.2020.08.016.

COMPETING INTERESTS

All authors declare no conflict of interest.

AUTHORS' CONTRIBUTIONS

A.C. run the experiments, analysed the data, drafted the work. C.D., acquired and analysed data, revised the manuscript. V.L. and L.R. developed the in vitro aggregation assays and acquired data. M.E. and D.M.M. performed the TCGA analysis. L.Lamant and L.Lanfrancone chose and prepared the DNA patient samples. A.P. and G.F. proposed and prepared the cellular and *in vivo* models. F.B. and J.T. acquired and analysed bisulfite pyrosequencing data. C.E., J.R. and P.B.A. designed the study acquired and analysed data, supervised the study, acquired funds and drafted the manuscript.

Figure Legends.

Figure 1. Analysis of CpG methylation of *PCDBH15* in melanoma cell lines and patient samples and re-expression after 5azadC treatment of WM266-4 cell line.

(A) The percentage of DNA methylation of each CpG in *PCDHB15* was analysed by bisulfite conversion followed by pyrosequencing of the CpGs indicated as black dots. CpGs on the sequence but not amplified in pyrosequencing are indicated as dotted lines. The CpGs of the Illumina 450K array are indicated by an asterisk: for *PCDHB15*, cg27328673, cg23974473 and cg09135656 at +566, +610 and +664pb from the TSS, respectively.

(B-C) The DNA methylation mean level of *PCDHB15* (B) was measured in two pairs of cell lines originating from two different patients, WM115/WM266-4 cells and WM983A/WM983B (B), as well as in genomic DNA obtained from 27 patient samples, primary (n=18) or metastases (n= 9) (C). Data are presented as boxplot of the median DNA methylation percentage of CpGs in black (6 CpGs for *PCDHB15)*. The

median values for primary and metastasis samples are 61.5% and 71.6%, respectively, Jarque-Bera's test to analyse normality, Fisher's test to analyse variances and Student t-test were performed, n.s= not significant, *=p<0.05, ** = p<0.01, *** = p<0.001.
(D) Normalized beta values for the Illumina probes of DNA methylation for primary melanoma (PRM), lymph node metastasis (LNM) and distant organ metastasis (DOM) from TCGA-SKCM DNA methylation data of PCDHB15 were summarized as a heatmap. A violin plot was used to highlight CpGs identified as hypermethylated in metastatic cell lines in our previous study. Differential DNA methylation was assessed by the Wilcoxon Rank-Sum test. All p-values from multiple comparisons (>50 tests) were corrected using the False discovery rate (FDR) method. *=p<0.05. Transcription factor clusters from Transcription Factor ChIP-seq Clusters (340 factors, 129 cell types) from ENCODE 3 were indicated as black/grey scale.
WM266-4 cells were treated with increasing concentrations of 5azadC daily during 72h (d1, d2, d3). (E) At day 4, DNA methylation of *PCDHB15* at exon 1 was measured by pyrosequencing (n=2 for WM266-4 and WM115 cells; n=3 for 5azadC-treated cells). The box plots show the percentage of DNA methylation of the analyzed CpGs (from panel A). (F) The mRNA quantification of *PCDHB15* by RT-qPCR was performed at day 7, using the TBP gene as reference gene and normalized according to the expression level found in the WM266-4 cells (n=4, SEM are shown). Fisher's test to analyse variances and Student t-test were performed , ns = not significant, * = p< 0.05, ** = p<0.01, *** = p<0.001.

Figure 2. Characterization of PCDHB15 overexpressing clones.

(A) Western blot analysis of endogenous PCDHB15 in WM115 and WM266-4 cells and (B) of the overexpression of the PCDHB15 construct in WM266-4 cells, mock (transfected with the empty pCMV6 vector), clone 8, 12 and 13, revealed by the antibody against PCDHB15 or against DDK (for the constructs only). The Western blot is representative of n=3. Beta-actin was used as loading control (bottom).
(C) PCDHB15 mRNA quantification by RT-qPCR (on n=3 biologically independent experiments, ANOVA test, *: p < 0,05; **:p < 0,01. ***: p < 0,001). The value in WM266-4 cells was considered as 1.
(D) Cell surface expression of PCDHB15 measured by immunolabeling and flow cytometry. Black and white histograms display the cell surface fluorescence associated with PCDHB15 and isotypic control labeling, respectively.

Figure 3. 3D aggregation of WM266-4 cells is impaired by PCDHB15 overexpression.

The formation of aggregates of WM266-4 cells (WT), control cells (mock) and PCDHB15 overexpressing cells (clones 8, 12 and 13) was monitored by brightfield time-lapse videomicroscopy. (A) The images show representative aggregates at 0, 5, 15 and 20 h after the experiment onset. Pink lines delineate the maximal aggregate areas. Green lines delineate empty areas that are subtracted in the total area calculation. (B) The normalized area of the aggregates is reported at each time. The reported values are the mean of at least 6 individual aggregates analyzed in three independent experiments.

Figure 4. PCDHB15 overexpression in WM266-4 cells impairs 3D cell invasion.

The invasion ability of WM266-4 cells (WT), control cells (mock) and PCDHB15-overexpressing cells (clones 8, 12 and 13) was measured using a 3D-invasion assay in collagen matrix. Images are representative of at least 6 spheroids per condition before (A) and after (B) 24h invasion. The initial sizes of each spheroid (C) and their invasion index at 24h (D) are reported as histograms. Means and SEM were calculated from 6 spheroids measured in three independent experiments. Jarque-Bera's test to analyse normality, Fisher's test to analyse variances and Student t-test were performed; P-value<0.05, **: P-value<0.01. ***: P-value<0.001.

Figure 5. PCDHB15 overexpression impairs WM266-4 lung metastasis formation *in vivo*.

WM-266-4 overexpressing PCDHB15 (clone 8, 12, 13) or mock cells (with void vector) were injected in the tail vein (IV) of SCID mice. Lungs were recovered for immunohistochemical analysis 21 days after injection. (A) A representative image of the stained lung is shown for each group. Black arrows indicate metastases. Plots representing the median of number (B) and size (C) of metastases on one slice for each mouse are shown**.** n=15 for mock, clone 8, clone 12; n=14 for clone 13. Medians and SEM are shown. Mann-Whitney test; **P value < 0.01, ***P value < 0.001.

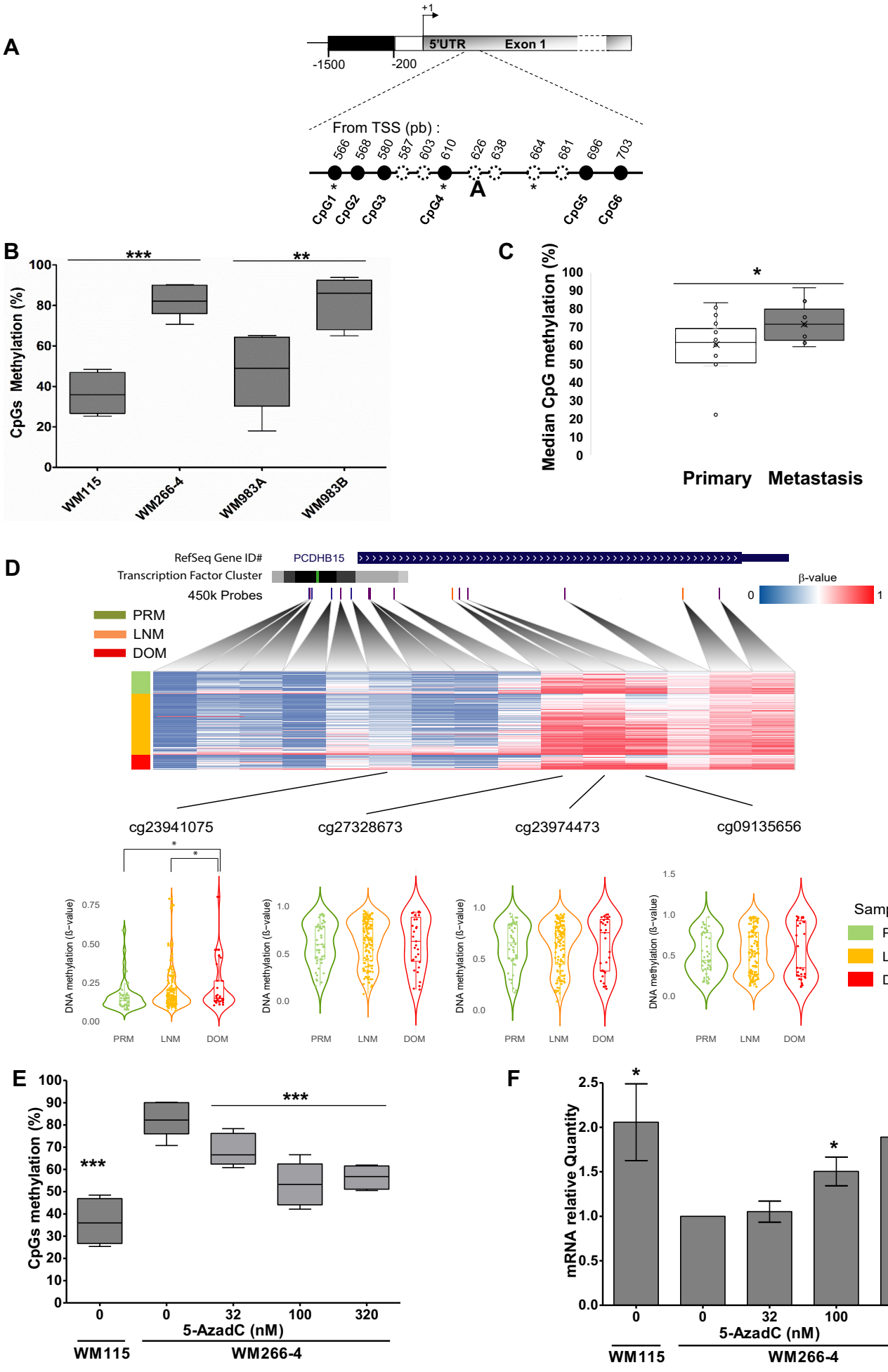
A
+1
5'UTR
Exon 1
-1500
-200
From TSS (pb) :
566
568
580
587
603
610
626
638
664
681
696
703
CpG1
CpG2
CpG3
CpG4
A
CpG5
CpG6
B
CpGs Methylation (%)
WM115
WM266-4
WM983A
WM983B
C
Median CpG methylation (%)
Primary
Metastasis
D
RefSeq Gene ID#
PCDHB15
Transcription Factor Cluster
450k Probes
β-value
PRM
LNM
DOM
cg23941075
cg27328673
cg23974473
cg09135656
DNA methylation (β-value)
Samples
E
CpGs methylation (%)
5-AzadC (nM)
WM115
WM266-4
F
mRNA relative Quantity
5-AzadC (nM)
WM115
WM266-4

Figure 1

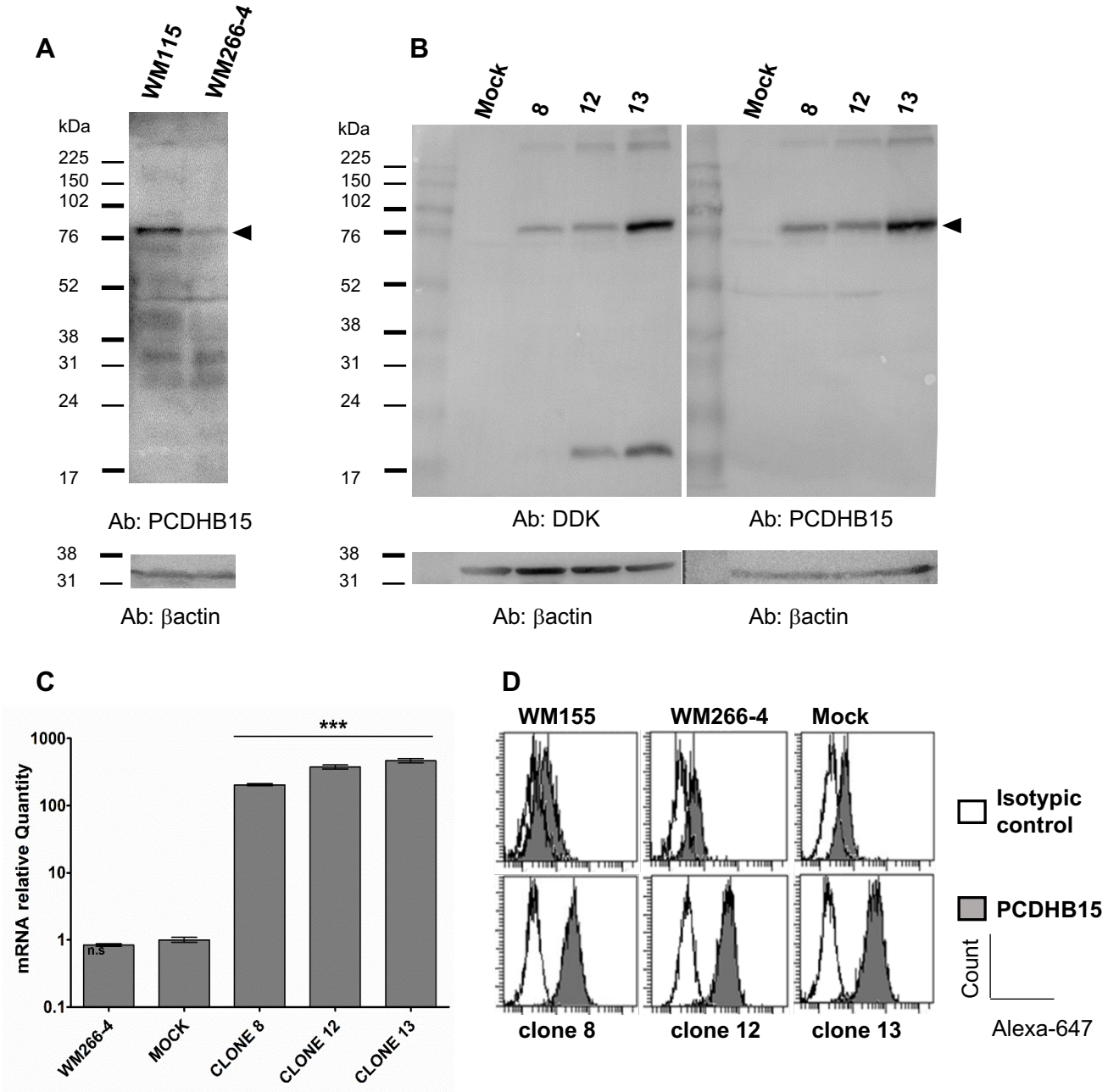
A
WM115
WM266-4
kDa
225
150
102
76
52
38
31
24
17
Ab: PCDHB15
38
31
Ab: βactin
B
Mock
8
12
13
Mock
8
12
13
kDa
225
150
102
76
52
38
31
24
17
Ab: DDK
Ab: PCDHB15
38
31
Ab: βactin
Ab: βactin
C
***
mRNA relative Quantity
1000
100
10
1
0.1
n.s
WM266-4
MOCK
CLONE 8
CLONE 12
CLONE 13
D
WM155
WM266-4
Mock
clone 8
clone 12
clone 13
Isotypic control
PCDHB15
Count
Alexa-647

Figure 2

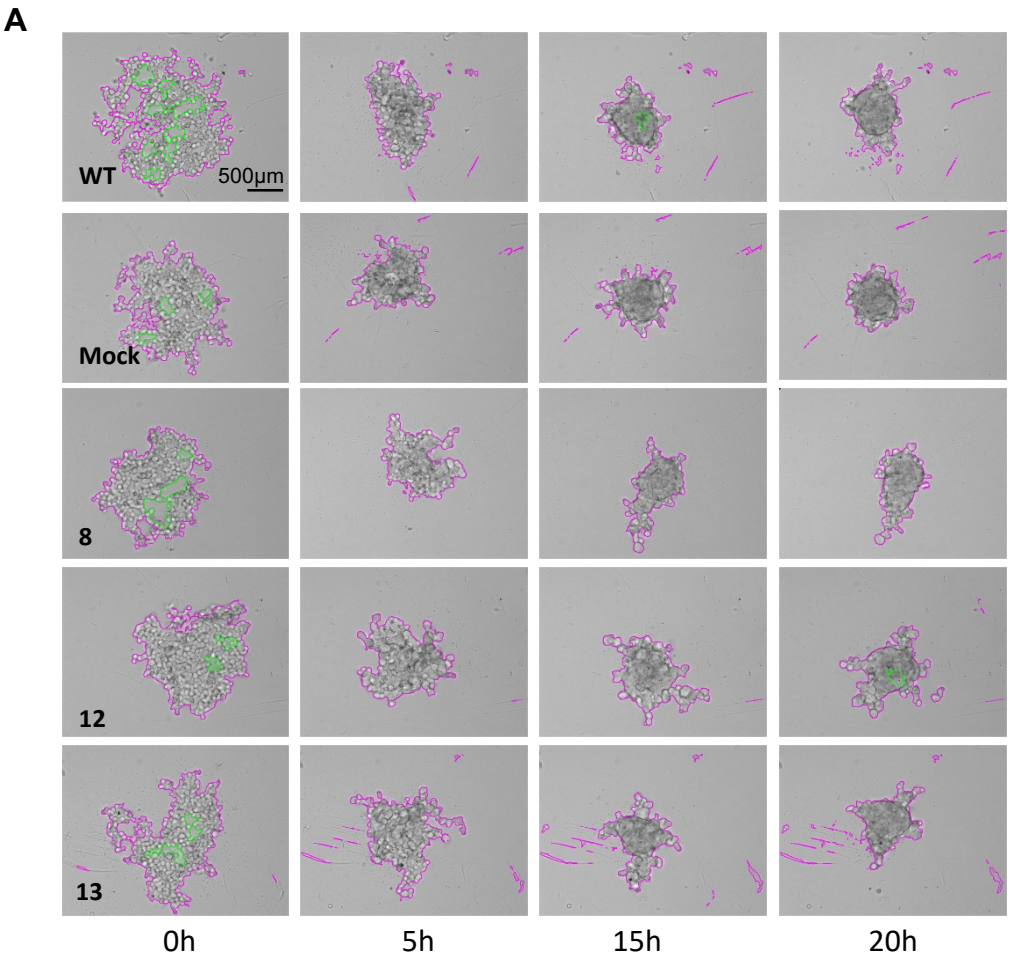
A
WT
500μm
Mock
8
12
13
0h
5h
15h
20h
B
Normalized Area
1.0
0.9
0.8
0.7
0.6
0.5
0.4
0.3
0
5
10
15
20
TIME (hours)
Mock
8
12
13

Figure 3

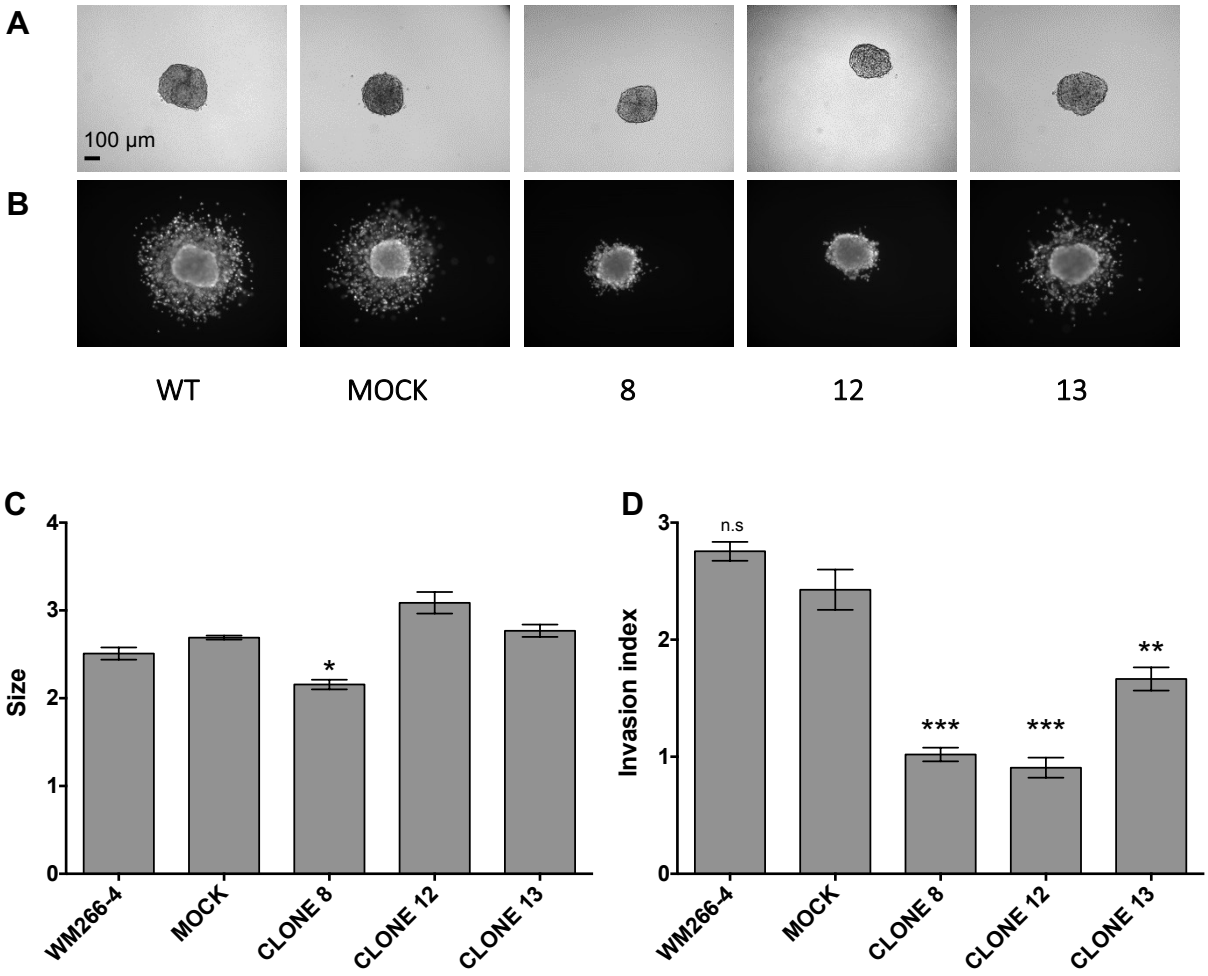
A
100 µm
B
WT
MOCK
8
12
13
C
Size
4
3
2
1
0
*
WM266-4
MOCK
CLONE 8
CLONE 12
CLONE 13
D
Invasion index
3
2
1
0
n.s
***
***
**
WM266-4
MOCK
CLONE 8
CLONE 12
CLONE 13

Figure 4

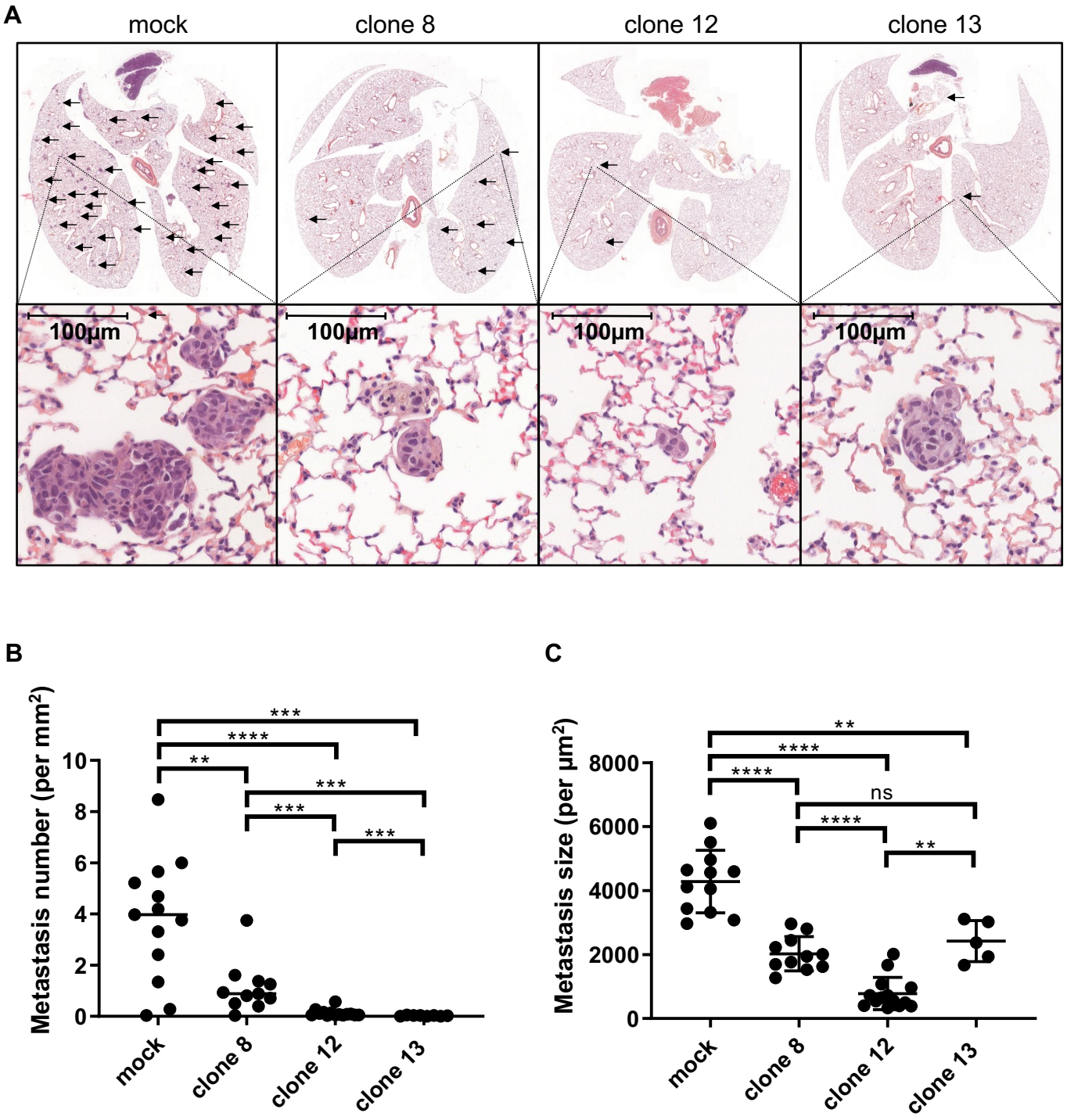
A
mock
clone 8
clone 12
clone 13
100μm
100μm
100μm
100μm
B
Metastasis number (per mm²)
0
2
4
6
8
10
***
****
**
***
***
***
mock
clone 8
clone 12
clone 13
C
Metastasis size (per μm²)
0
2000
4000
6000
8000
**
****
****
ns
****
**
mock
clone 8
clone 12
clone 13

Figure 5